

Reduced IGF-1 Signaling Delays Age-Associated Proteotoxicity in Mice

Ehud Cohen,^{1,7} Johan F. Paulsson,² Pablo Blinder,³ Tal Burstyn-Cohen,⁴ Deguo Du,² Gabriela Estepa,¹ Anthony Adame,⁵ Hang M. Pham,⁵ Martin Holzenberger,⁶ Jeffery W. Kelly,² Eliezer Masliah,⁵ and Andrew Dillin^{1,*}

¹Howard Hughes Medical Institute, Glenn Center for Aging Research, Molecular and Cell Biology Laboratory, The Salk Institute for Biological Studies, 10010 North Torrey Pines Road, La Jolla, CA 92037, USA

²Department of Chemistry and Molecular and Experimental Medicine and The Skaggs Institute of Chemical Biology, The Scripps Research Institute, 10550 North Torrey Pines Road, La Jolla, CA 92037, USA

³Department of Physics, University of California, San Diego, 9500 Gilman Drive, La Jolla, CA 92093, USA

⁴Molecular Neurobiology Laboratory, The Salk Institute for Biological Studies, 10010 North Torrey Pines Road, La Jolla, CA 92037, USA

⁵Department of Neurosciences, University of California, San Diego, 9500 Gilman Drive, La Jolla, CA 92093, USA

⁶INSERM and Université Pierre-et-Marie-Curie, UMRS 938, Hôpital Saint-Antoine, 75571 Paris 12, France

⁷Present address: Department of Biochemistry and Molecular Biology, the Institute for Medical Research Israel-Canada, The Hebrew University Medical School, Ein Kerem, Jerusalem 91120, Israel

*Correspondence: dillin@salk.edu

DOI 10.1016/j.cell.2009.11.014

SUMMARY

The insulin/insulin growth factor (IGF) signaling (IIS) pathway is a key regulator of aging of worms, flies, mice, and likely humans. Delayed aging by IIS reduction protects the nematode *C. elegans* from toxicity associated with the aggregation of the Alzheimer's disease-linked human peptide, A β . We reduced IGF signaling in Alzheimer's model mice and discovered that these animals are protected from Alzheimer's-like disease symptoms, including reduced behavioral impairment, neuroinflammation, and neuronal loss. This protection is correlated with the hyperaggregation of A β leading to tightly packed, ordered plaques, suggesting that one aspect of the protection conferred by reduced IGF signaling is the sequestration of soluble A β oligomers into dense aggregates of lower toxicity. These findings indicate that the IGF signaling-regulated mechanism that protects from A β toxicity is conserved from worms to mammals and point to the modulation of this signaling pathway as a promising strategy for the development of Alzheimer's disease therapy.

INTRODUCTION

Most cases of Alzheimer's disease (AD) exhibit sporadic onset during the seventh decade of life or later, whereas the fewer mutation-linked, familial cases typically manifest during the fifth decade. These temporal features, common to numerous neurodegenerative diseases, define aging as the major risk factor for the development of these maladies (Amaducci and Tesco, 1994). The insulin/insulin-like growth factor (IGF) signaling (IIS) pathway regulates stress resistance, aging and is a life span determinant. IIS reduction results in stress-resistant, long-lived

worms (Kenyon et al., 1993), flies (Tatar et al., 2001), and mice (Blüher et al., 2003; Holzenberger et al., 2003) and correlates with increased longevity of humans (Flachsbart et al., 2009; Suh et al., 2008; Willcox et al., 2008). Delayed aging, by IIS reduction, protects worms from proteotoxicity associated with the aggregation of the Huntington's disease-associated polyQ peptide (Morley et al., 2002) and the AD-linked human A β peptide (Cohen et al., 2006). However, little is known about whether this protection from proteotoxicity is conserved from worms to mammals, and what protective mechanisms may be operating.

A β originates from the endoproteolysis of the amyloid precursor protein (APP) (Glennner and Wong, 1984; Selkoe, 2004). The serine protease BACE (*beta* amyloid cleaving enzyme) cleaves APP (Farzan et al., 2000), followed by an intramembrane cleavage of the resulting fragment by presenilin1 (PS1), an active component of the γ -secretase proteolytic complex (Wolfe et al., 1999). These events release the A β family of aggregation-prone peptides, including A β ₁₋₄₀ and the highly amyloidogenic A β ₁₋₄₂. Although compelling data indicate that A β aggregation triggers AD, the mechanism leading to the development of the disease is unclear (Selkoe, 2004). Recent studies suggest that it is not fibrils, but small A β oligomers lead to toxicity in AD model organisms (Cohen et al., 2006; Lesne et al., 2006) and to AD in humans (Haass and Selkoe, 2007; Shankar et al., 2008).

In the *C. elegans* A β model (A β worms [Link, 1995]), the protection from human A β ₁₋₄₂ proteotoxicity conferred by IIS reduction is dependent upon two transcription factors, heat shock factor 1 (HSF-1), which regulates A β disaggregation, and DAF-16 (ortholog to FOXO in mammals), which facilitates the formation of larger, less toxic A β aggregates. Accordingly, A β worms protected from A β toxicity by reduced IIS accumulate more large A β aggregates and have fewer oligomers than did their unprotected counterparts with normal IIS (Cohen et al., 2006).

Although reduced IGF signaling extends the life span of mice (Holzenberger et al., 2003), IGF-1 infusion protects from A β toxicity (Carro et al., 2002, 2006), raising the query of whether

IGF signaling reduction or activation protects from A β toxicity. To address this question, we created an AD mouse model with reduced IGF signaling by crossing a well-established AD transgenic mouse model (Jankowsky et al., 2001) with long-lived mice harboring only one *Igf1r* gene copy (*Igf1r*^{+/-} mice) (Holzenberger et al., 2003).

RESULTS

Creation of Mice with AD Transgenes in the Context of Reduced IGF-1R Signaling

Igf1r is the mammalian ortholog of the sole worm insulin/IGF receptor *daf-2* (Kimura et al., 1997). *Igf1r*^{+/-} mice exhibit reduced IGF-1 signaling, are long-lived, oxidative stress resistant, and have reduced body size (Holzenberger et al., 2003). The AD mouse model expresses two AD-linked mutated transgenes, APP_{swe} (a humanized mouse APP that contains the human A β peptide sequence) and human presenilin-1 Δ E9, both driven by the mouse prion protein promoter (hereafter referred to as AD mice) (Jankowsky et al., 2001). The expression of these transgenes results in the production of human A β amyloid, plaque formation in the brain, and slow, progressive AD-like symptoms (Jankowsky et al., 2004). The AD-like mice also exhibit age-onset behavioral impairments, analogous to other AD murine models (Reiserer et al., 2007). The AD model is less aggressive than other AD models, exhibiting appearance of A β plaques in the brain at 6–7 months of age (Jankowsky et al., 2004). The slow onset of AD-like symptoms allows for the perturbation of IIS to examine its role in the age onset requirements of the AD-like syndrome.

To equalize the genetic background of our mice, we first backcrossed both the AD and *Igf1r*^{+/-} mouse strains with wild-type 129 females for three generations, followed by four intercrosses between the AD and *Igf1r*^{+/-} mice. Crossing *Igf1r*^{+/-} with the AD mice generated offspring of four genotypes (Figure 1A): The original parental genotypes, (1) heterozygous *Igf1r*^{+/-} (*Igfr*^{+/-}) and (2) AD mice, which served as internal controls (AD). (3) Congenic siblings that age naturally due to two *Igf1r* gene copies but carrying neither of the AD transgenes. These animals served as negative internal controls for asymptomatic AD-like disease and natural IGF-1 signaling (WT). Finally, (4) mice harboring both AD transgenes and only one *Igf1r* gene copy served as the experimental group of focus (AD;*Igf1r*^{+/-}).

Quantitative polymerase chain reaction (PCR) analysis revealed that the expression levels of the APP_{swe} transgene were nearly identical in brains of AD and AD;*Igf1r*^{+/-} mice (Figures S1A–S1E available online), indicating that IGF signaling reduction does not effect the expression of the prion protein promoter-driven transgenes. The levels of monomeric A β and of the C-terminal APP fragment (APP CTF) were also very similar in AD and AD;*Igf1r*^{+/-} mice (Figures S1F and S1G). Similarly, reduced IGF signaling did not affect the endogenous α and β secretases (ADAM17 and BACE, respectively) in mouse brains of all genotypes (Figure S1H). Together these results indicate that IGF signaling reduction affected neither the transgene expression nor the levels of the endogenous APP processing enzymes or their activity. As expected, both *Igf1r*^{+/-} and AD;*Igf1r*^{+/-} mice were smaller compared with their littermates carrying two

Igf1r copies, indicating reduced IGF-1R signaling (Figure S2A) (Holzenberger et al., 2003).

Reduced IGF-1R Signaling Reduces the Behavioral Deficits of AD Mice

Age-onset memory deficiency and impairment of orientation and locomotion are associated with A β production in numerous AD murine models (Jensen et al., 2005; King and Arendash, 2002; Westerman et al., 2002). We evaluated whether reduced IGF-1 signaling protects mice from A β -associated behavioral impairments using several behavioral assays. As an initial analysis, we used eight animals per genotype and followed their performance in the Morris water maze test at 3, 6, 9, and 12 months of age, and found the greatest differences among AD, AD;*Igf1r*^{+/-} animals and their littermate controls at the 9 and 12 month time points (Figures S2B and S2C). At 16 months we observed mortality in the AD group that was not present in the AD;*Igf1r*^{+/-} mice (data not shown). Thus, we refined our behavioral analysis to the 11–15 month of age using a larger cohort of animals.

We measured the learning ability of mice using a Morris water maze with a cued (visible) platform for four consecutive days. As previously reported for other AD model mice (Blanchard et al., 2008; Westerman et al., 2002), the AD mice did not exhibit a learning deficiency compared to their age-matched WT, *Igf1r*^{+/-}, and AD;*Igf1r*^{+/-} counterparts (Figure 1B, $p > 0.05$). In order to test orientation aptitude, we removed the cue from the platform and recorded the latency time required for mice to locate the submerged platform for four consecutive days. At days 2, 3, and 4 of the experiment, AD mice required a significantly ($p < 0.05$) longer time to find the hidden platform compared to their WT, *Igf1r*^{+/-}, and AD;*Igf1r*^{+/-} counterparts (Figure 1C). This indicates that, like other mouse AD models (Jensen et al., 2005; King and Arendash, 2002; Westerman et al., 2002), orientation capabilities of AD animals are impaired (swim velocities were nearly identical for all genotypes; Figure S2D). Lastly, we tested memory skills by removing the platform from the water maze and recording the number of the crosses of the previous platform location (probe trial). AD mice crossed the platform's previous location significantly ($p < 0.05$) fewer times than their WT, *Igf1r*^{+/-}, and most importantly AD;*Igf1r*^{+/-} counterparts, indicating impaired memory. The observation that AD;*Igf1r*^{+/-} animals crossed the previous platform location at similar frequencies compared to WT and *Igf1r*^{+/-} animals suggests partial memory restoration (Figure 1D).

Next, we tested the effect of reduced IGF-1 signaling on the motor skills of AD model mice using a Rota-Rod assay. Much like the orientation and memory tests, AD mice performed significantly less well than their age-matched WT, *Igf1r*^{+/-}, and AD;*Igf1r*^{+/-} counterparts in this assay (Figure 1E, $p < 0.05$).

Collectively, the behavioral data revealed that AD mice have impaired orientation and memory performance as well as locomotion impairment that can be delayed by reduced IGF-1 signaling.

Reduced IGF-1R Signaling Reduces Inflammation and Neuronal Loss in AD Mice

We asked whether the appearance of biological markers associated with AD-like disease in mice was also delayed by reduced

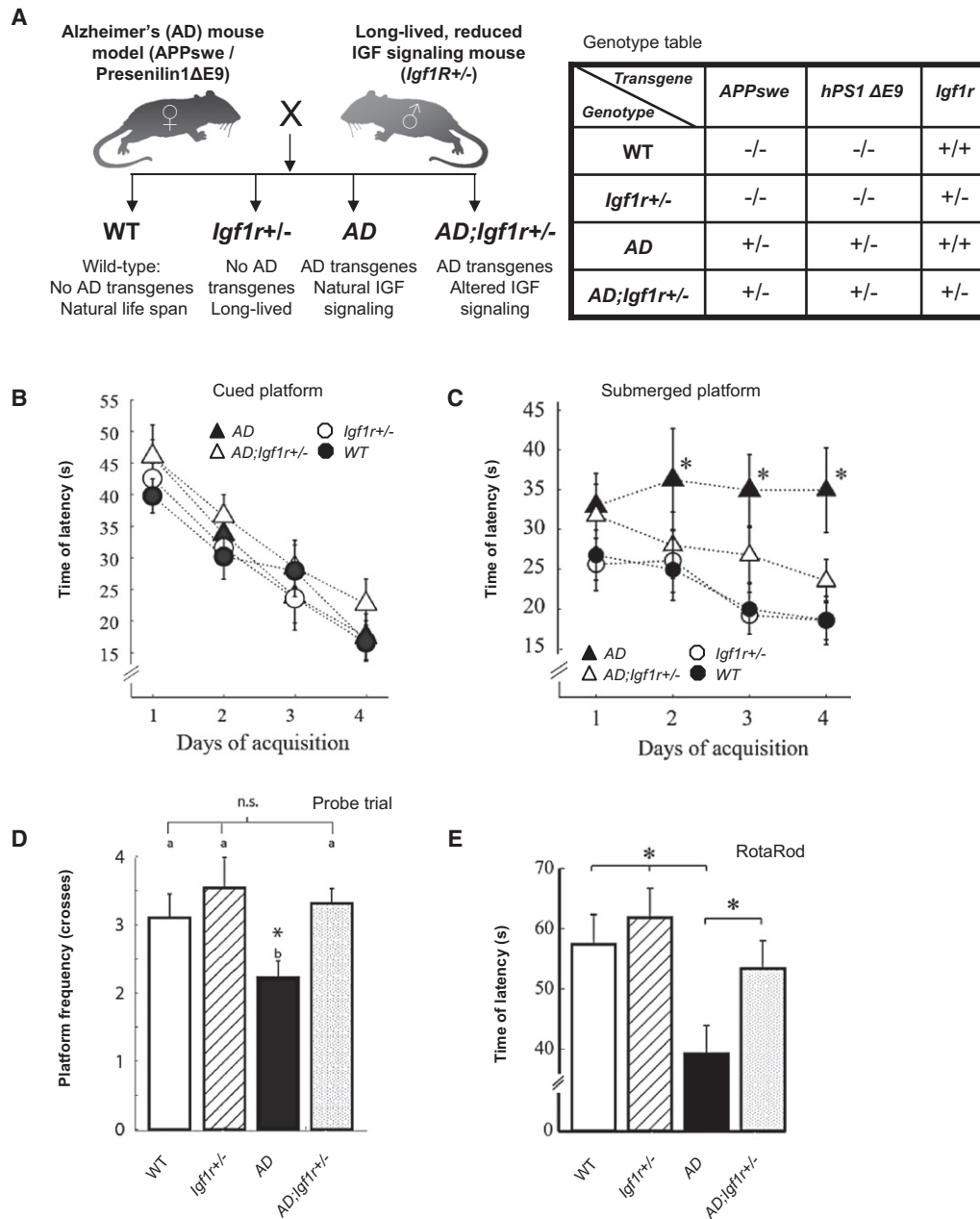


Figure 1. Reduction of IGF Signaling Protects Mice from A β -Associated Behavioral Impairments

(A) Long-lived mice carrying one *Igf1r* copy were crossed with transgenic Alzheimer's disease (AD) model mice harboring two AD-linked mutated genes, APP^{swe} (containing the human A β sequence) and PS1 Δ E9 to obtain offspring of four genotypes: (1) wild-type, harboring two *Igf1r* copies and no AD-linked transgenes (WT), (2) long-lived mice with one *Igf1r* copy and no AD-linked transgenes (*Igf1r*^{+/-}), (3) AD model mice with two *Igf1r* copies and both AD-linked transgenes (AD), and (4) mice that harbor one *Igf1r* copy and both AD-linked transgenes (AD;*Igf1r*^{+/-}).

(B) Latency time for reaching the cued platform significantly decreased through the acquisition sessions ($p = 0$, $F = 35.49$, $df = 3$) in mice of all genotypes ($p > 0.05$, $F = 1.84$, $df = 3$, $n = 8, 15, 16, 18$ for AD, AD;*Igf1r*^{+/-}, WT, and *Igf1r*^{+/-}, respectively), suggesting no impairment of learning.

(C) Significant differences were observed among AD mice and their counterparts of the other genotypes in the submerged platform test ($p = 5E-4$, two-way analysis of variance [ANOVA], $F = 7.71$, $df = 3$) and across the acquisition days ($p = 0.032$, $F = 2.97$, $df = 3$, $n = 8, 15, 16, 18$ for AD, AD;*Igf1r*^{+/-}, WT, and *Igf1r*^{+/-}, respectively). AD mice searched for a longer period of time ($p < 0.05$, Fisher LSD) for the submerged platform. No difference was observed among the three other genotypes.

(D) AD;*Igf1r*^{+/-} animals crossed the previous platform location significantly ($p = 0.024$, Kruskal-Wallis, $\chi^2 = 9.38$, $df = 3$) more times than their AD counterparts.

(E) Mice older than the age of plaque formation of all genotypes were tested in a Rota Rod task. Animals of the different genotypes significantly differed in their performance ($p < 0.01$, one-way ANOVA, $df = 3$, $F = 4.25$; $n = 31, 32, 29$, and 28 individuals for AD, AD;*Igf1r*^{+/-}, *Igf1r*^{+/-}, and wild-type, respectively). AD mice performed worst among the four genotypes whereas AD;*Igf1r*^{+/-} mice where partially rescued because they performed significantly better than AD animals ($p < 0.05$, Tuckey LSD). No statistical difference appeared between AD;*Igf1r*^{+/-} animals and the two control genotypes. In all behavioral tests, 11- to 15-month-old mice were tested and age-match controlled. Error bars represent mean and standard error of the mean (\pm SEM).

12-13 month old, Astrocytosis (GFAP)

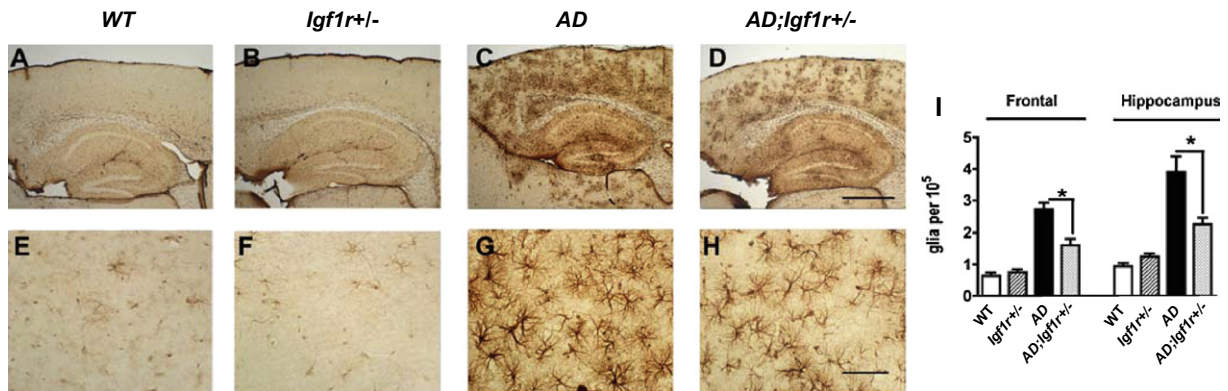


Figure 2. Reduced IGF Signaling Reduces A β -Associated Neuroinflammation

(A–H) Immunohistochemistry using GFAP antibody indicated reduced astrocytosis in brain sections of 12- to 13-month-old *AD;Igf1r*^{+/-} mice (D and H) compared with age-matched *AD* mice (C and G).

(I) Image analysis confirmed the significance of the GFAP signal difference (six mice per genotype and 3 sections per animal were analyzed, $p < 0.05$; error bars represent mean \pm SEM).

IGF signaling. First we tested whether reactive astrocytosis, indicative of neuroinflammation, associated with AD in humans (Mancardi et al., 1983), and with A β aggregation in brains of AD model mice (Wirhth et al., 2008), was reduced in *AD;Igf1r*^{+/-} animals. Utilizing glial fibrillary acidic protein (GFAP) antibodies, which recognize activated astrocytes (Mancardi et al., 1983), we found notably less activated astrocytes in the brains of *AD;Igf1r*^{+/-} mice compared with age-matched *AD* mice (Figure 2). This reduction was apparent both in the cortex and hippocampus (Figure 2I), indicating that neuroinflammation is reduced in *AD;Igf1r*^{+/-} mice compared with age-matched *AD* mice. Interestingly, whereas the GFAP signal observed in cortices of *AD* mice was largely diffuse, cortical GFAP staining of *AD;Igf1r*^{+/-} mice appeared to be focal (compare Figures 2C and 2D), suggesting that neuroinflammation within *AD;Igf1r*^{+/-} brains is confined to smaller areas than in the brains of *AD* animals.

Neuronal loss is another hallmark of AD in humans (Scheff et al., 1990) and AD model mice (Maslah and Rockenstein, 2000). We used direct stereological visualization and NeuN immunoreactivity, a marker of neuronal density that declines in *AD* mice, and found higher NeuN immunoreactivity in the cortices of 12- to 13-month-old *AD;Igf1r*^{+/-} mice compared to their age-matched *AD* counterparts (Figure 3). This indicates that reduced IGF signaling protects from neuronal loss. Similar neuronal losses were observed in young (4–5 months of age) and in old (16–17 months) *AD* but not in *AD;Igf1r*^{+/-} mice when compared to age-matched control genotypes (Figure S3).

Reduced synaptic density is an additional hallmark and probably causative of AD (Hamos et al., 1989). Thus, we used the synaptic marker synaptophysin to compare synaptic densities in frontal and hippocampal brain regions of 12- to 13-month-old mice of all genotypes (Hamos et al., 1989) and found significantly lower synaptic densities in both brain regions (Figures 3J and 3K, respectively) of *AD* animals compared with their *AD;Igf1r*^{+/-} counterparts. These observations confirm that IGF

signaling reduction protects mice from A β -associated neuronal loss.

Reduced IGF Signaling Promotes the Formation of Densely Packed Aggregates

To explore the mechanism underlying the protection toward behavioral deficiencies conferred by reduced IGF signaling, as well as the protection from inflammation and neuronal loss in mice ectopically expressing mutated AD-linked transgenes, we investigated the nature of A β assemblies in brains of *AD* and *AD;Igf1r*^{+/-} mice. Immunohistochemistry (IHC) and A β antibodies (clone 6E10) were used to visualize A β plaques in brain sections of *AD* and *AD;Igf1r*^{+/-} mice (Figure S4). Consistent with previous results (Jankowsky et al., 2004), A β plaques could not be detected in brains of young mice (4–5 months old). A few plaques were observed in the brains of 8- to 9-month-old animals, whereas the number of plaques increased in the brains of 12- to 13-month-old *AD* and *AD;Igf1r*^{+/-} mice. No background staining was observed in brains of WT or *Igf1r*^{+/-} mice at any age examined (Figure S4). Thus, reduced IGF signaling has no apparent effect on the onset of plaque formation. Next we used the fluorescent dye Thioflavin-S to visualize amyloid within *AD* and of *AD;Igf1r*^{+/-} brains and found nearly identical amyloid load in cortex and hippocampus regions of both genotypes (Figure 4A, panel IX). (Colocalization of Thioflavin-S labeling with the signal of specific A β antibody [clone 82E1] confirmed the plaque specificity of Thioflavin-S; Figure S5A). Therefore, the kinetics of A β plaque appearance as well as the amyloid load did not appear to differ between *AD* and *AD;Igf1r*^{+/-} animals.

Closer inspection of the A β plaques analyzed by IHC revealed that plaques observed in the cortices of *AD;Igf1r*^{+/-} animals are smaller and more condensed than those detected in the cortices of their age-matched *AD* counterparts (Figure S4, 12–13 months, insets). To compare the plaque compaction in the mouse brains,

12-13 month old, Neural density (NeuN)

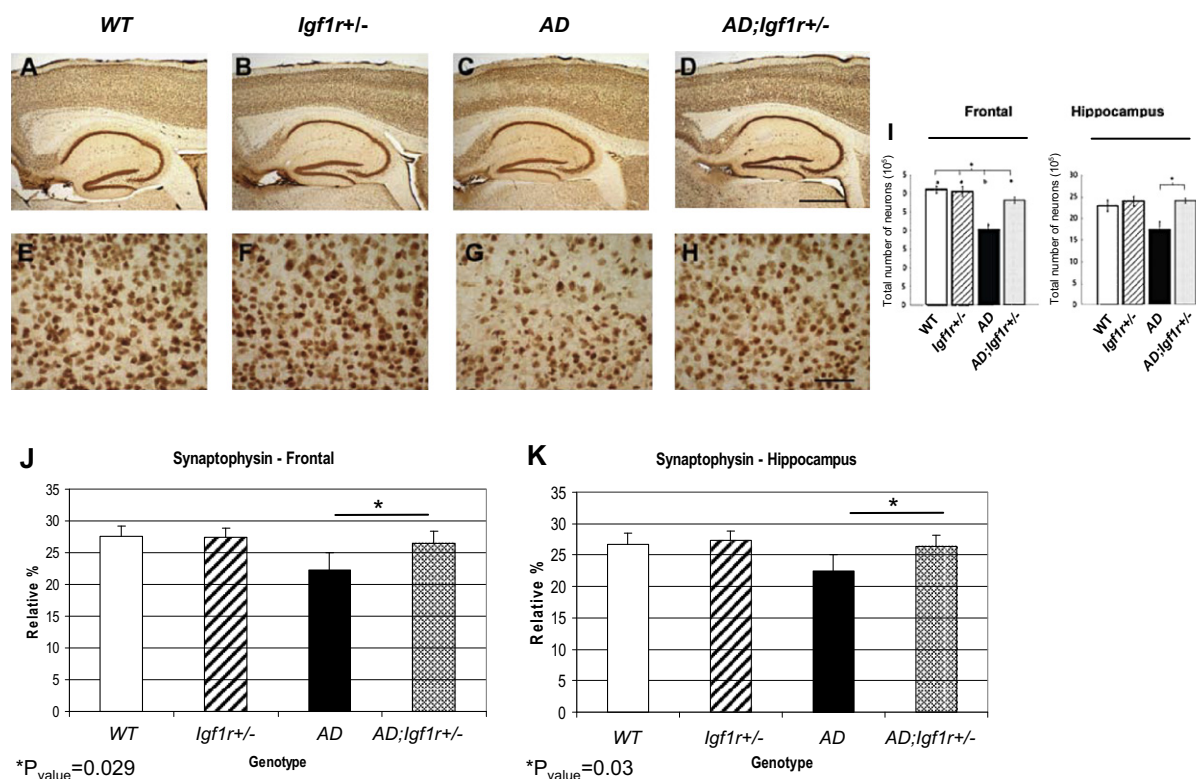


Figure 3. Reduced IGF Signaling Protects from A β -Associated Neuronal and Synaptic Loss

(A–H) Immunohistochemistry using NeuN antibody indicated that neural densities in the brains of 12- to 13-month-old *AD;Igf1r*^{+/-} (D and H), WT (A and E), and *Igf1r*^{+/-} (B and F) mice were comparable, while remarkable neuronal loss was observed in brains of age-matched AD animals (C and G).

(I) Image analysis of the NeuN signals indicated that neural density in both cortices and hippocampuses of AD animals was significantly lower compared with their age-matched WT counterparts (cortex: $p < 0.001$, one-way ANOVA, $F = 16.03$; hippocampus: $p < 0.05$, Kruskal-Wallis $\chi^2 = 9.36$, $df = 3$). No significant difference was observed among brains of *AD;Igf1r*^{+/-} and *Igf1r*^{+/-} mice (six mice per genotype and three sections per animal were analyzed).

(J and K) Immunohistochemistry using synaptophysin antibody revealed that *AD;Igf1r*^{+/-} mice exhibit significantly higher synaptic densities than their age-matched AD counterparts in both frontal (J) and hippocampal (K) brain regions (AD $n = 7$, *AD;Igf1r*^{+/-} $n = 5$). Error bars represent mean \pm SEM.

we used the highly specific A β antibody (clone 82E1 that recognizes processed A β) and measured the A β immunoreactive optical density (signal per area) in the different brains. Significantly higher A β immunoreactive optical densities were detected in brains of *AD;Igf1r*^{+/-} mice than in AD brains (Figure 4B, panel IX), suggesting higher compaction of the A β amyloid plaques in *AD;Igf1r*^{+/-} animals.

We also compared the protease sensitivity of plaques of AD and *AD;Igf1r*^{+/-} animals by treating brain sections of 12- to 13-month-old mice with 10 $\mu\text{g}/\text{ml}$ proteinase K prior to their labeling with A β antibody. A diffuse staining of A β plaques seen in AD brain slices compared to the *AD;Igf1r*^{+/-} brain slices (Figure S5B) suggested that plaques of *AD;Igf1r*^{+/-} animals are more protease resistant than those of AD mice.

To further analyze the amyloid plaque density, we used post-embedding immunoelectron microscopy, A β antibodies, and gold-labeled protein A. A β fibrils in the cortex of *AD;Igf1r*^{+/-} mice appeared to be more densely compacted than those of their AD counterparts (Figures 5A and S6A). (The lack of immu-

noreactivity in the brain sections of WT and *Igf1r*^{+/-} mice confirmed the specificity of the antibody; Figure S6B).

To quantify and compare the density of the amyloid plaques of AD and *AD;Igf1r*^{+/-} mouse brains, we developed an electron microscopy (EM) image-processing algorithm that identifies the gold particles conjugated to the A β antibodies (Figures S6C–S6F), sets a region of interest (ROI) around each particle, and determines the median signal density within the ROI after excluding the gold particle (Figures S6G–S6I). ROIs that contain dense structures will have a lower score value due to less bright pixels and more dark pixels (i.e., lower gray-scale value). Cortices of six 12- to 13-month-old AD mice and five *AD;Igf1r*^{+/-} mice were visualized by EM and 135 images (34,087 ROIs) of AD and 101 images (26,066 ROIs) of *AD;Igf1r*^{+/-} were automatically segmented and analyzed in an unbiased manner. The distributions of ROI median signal intensities indicate that plaques of *AD;Igf1r*^{+/-} mice were significantly ($p < 0.038$) denser than those of age-matched AD counterparts (Figure 5B). The possibility that antibody accessibility to plaques of AD and

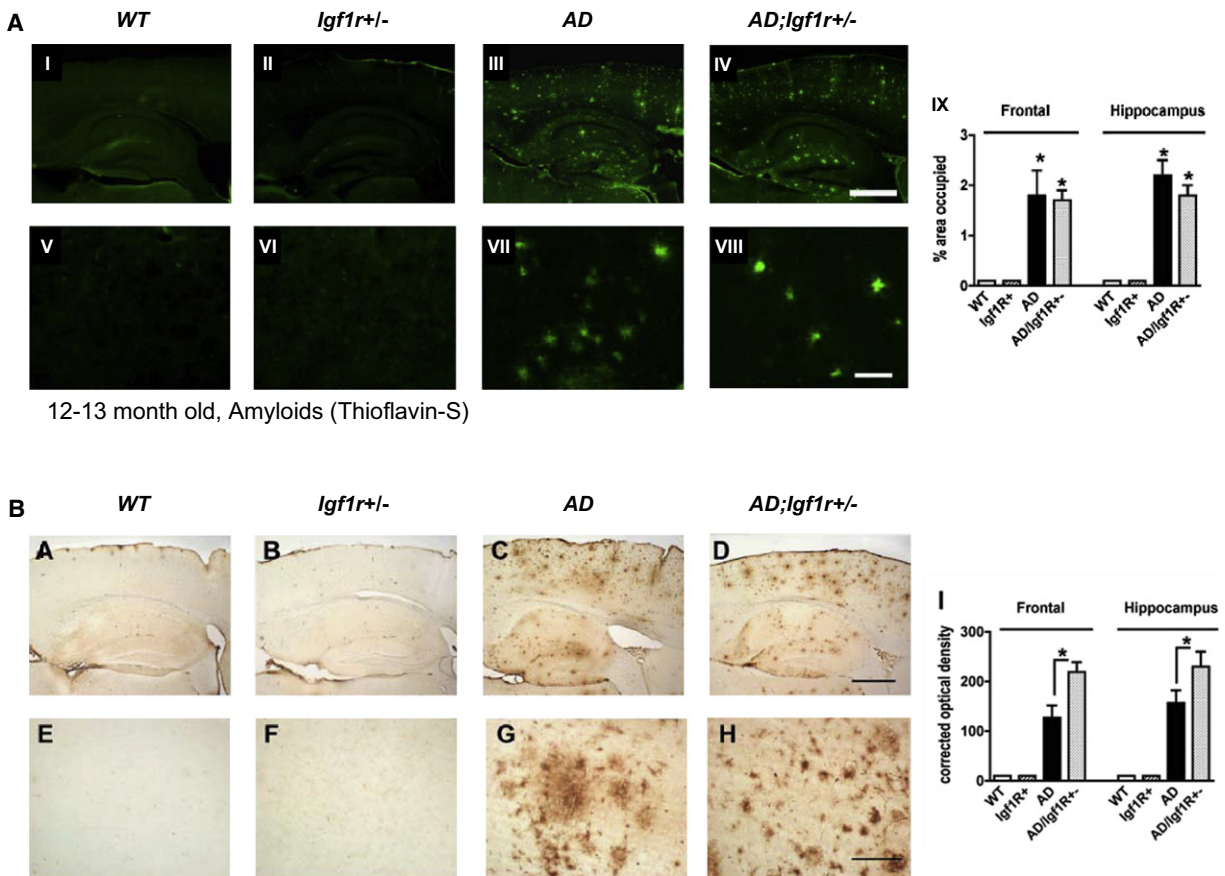


Figure 4. Reduced IGF Signaling Facilitates A β Hyperaggregation

(A) Thioflavin-S amyloid labeling showed similar A β plaque burden in brains of AD (panels III and VII) and AD;*Igf1r*^{+/-} animals (panels IV and VIII). Image analysis indicated that the Thioflavin-S signals are similar in brains of AD and AD;*Igf1r*^{+/-} mice, but significantly different from WT and *Igf1r*^{+/-} mice (panel IX). Six 12- to 13-month-old animals per genotype were analyzed.

(B) A β plaque signal density was measured using A β -specific antibody (82E1). The signal per area ratio in brains of AD;*Igf1r*^{+/-} animals (panels IV and VIII) was significantly higher (panel IX, $p < 0.05$) compared with brains of age-matched AD animals (panels III and VII), indicating higher plaque compaction in brains of AD;*Igf1r*^{+/-} mice (six mice per genotype and three sections per animal were analyzed; DG, dentate gyrus; NC, neocortex). Error bars represent mean \pm SEM.

AD;*Igf1r*^{+/-} brains differs was assessed by a second algorithm designed to measure the distance between each gold particle and its closest neighboring particle. This algorithm is based on the assumption that lower accessibility would result in sparse distribution and longer distances among the gold particles. Automatic processing of all plaque images of AD and AD;*Igf1r*^{+/-} showed no difference in distances (Figure S6J, $p > 0.54$), indicating similar antibody accessibilities.

The results obtained using light and electron microscopy suggest that reduced IGF signaling mediates the assembly of A β into more condensed amyloid plaques of lower toxicity. We used an in vitro kinetic aggregation assay (Cohen et al., 2006) to assess the relative total amounts of A β amyloid in equal volumes of brains of AD and AD;*Igf1r*^{+/-} mice. When proteinase K-treated and sonicated (fragments fibrils into a uniform size) brain homogenate is added to an A β ₁₋₄₀ aggregation reaction, the reduction in the time that it takes the aggregation reaction to reach 50% completion is proportional to the amount of A β amyloid fibrils in the tissue (Cohen et al., 2006) (D.D. and J.K.,

unpublished data). The amyloid load was assessed in 4- to 5-month-old and of 12- to 13-month-old AD and AD;*Igf1r*^{+/-} mouse brain homogenates (nine animals per genotype). While no significant difference in aggregate load could be detected among brain homogenates of young animals (4-5 months old, Figure S6K), brain extracts of 12- to 13-month-old AD;*Igf1r*^{+/-} mice exhibit a higher aggregate load reflected by a shorter t_{50} , (suggesting accelerated aggregation of A β ₁₋₄₀) relative to age-matched AD animals (Figure 5C; $p = 0.035$). These data demonstrate that there is more amyloids in an equal volume of 12- to 13-month-old AD;*Igf1r*^{+/-} brain relative to AD brain. These results are consistent with the light and electron microscopy data indicating that protected AD;*Igf1r*^{+/-} animals have more densely packed A β aggregates than AD animals.

Reduced IGF-1 Signaling Increases High-MW Aggregates and Reduces SDS-Soluble Aggregates

The hyperaggregation of A β by reduced IGF-1 signaling predicts lower residual amounts of nonaggregated A β and/or oligomeric

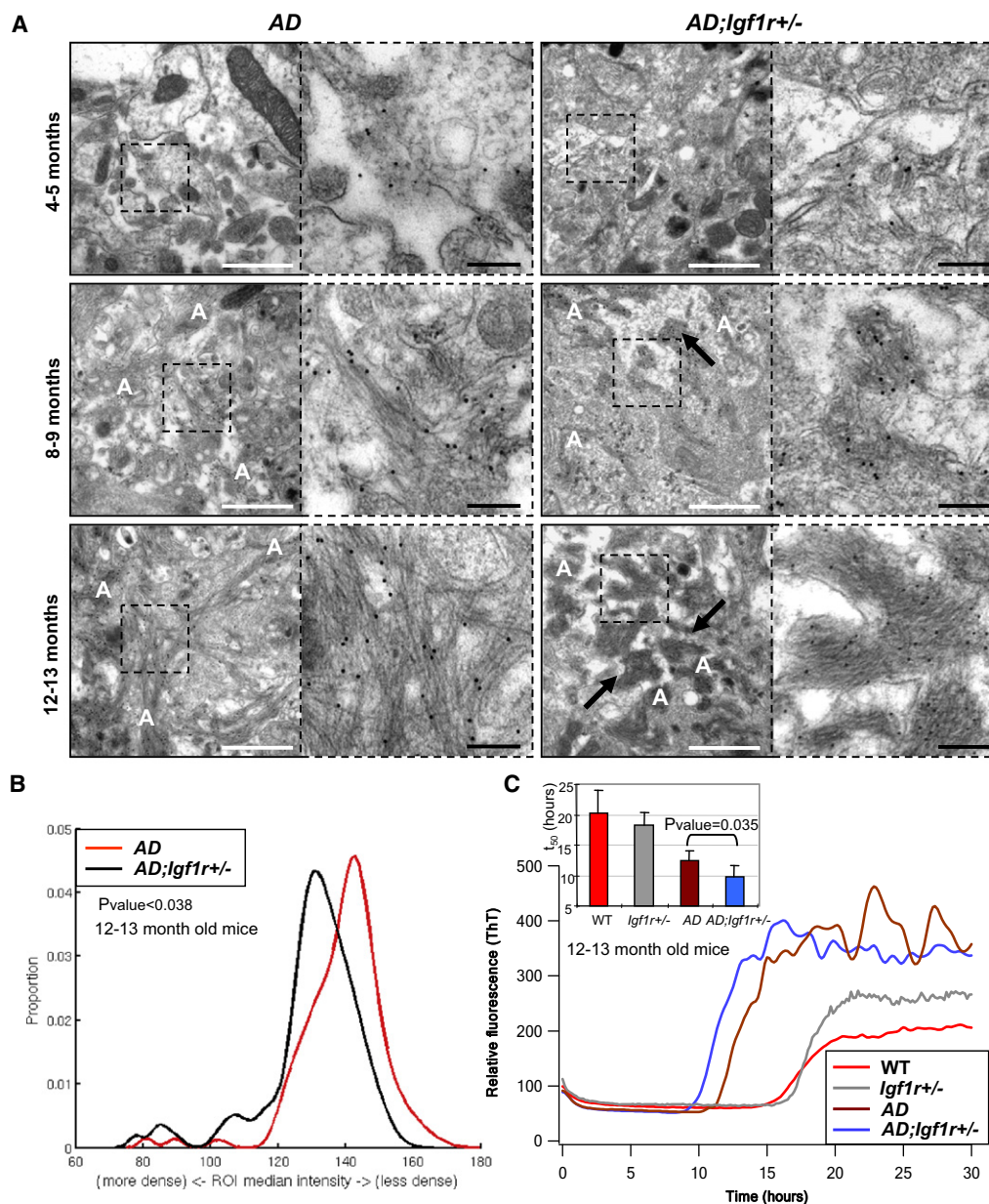


Figure 5. Electron Microscopy and In Vitro Kinetic Aggregation Assays Reveal Densely Packed A β Aggregates in the Brains of *AD;lgf1r^{+/-}* Mice

(A) Electron micrographs of immunogold-labeled A β amyloids in the cortex of *AD* and *AD;lgf1r^{+/-}* mouse brains at different ages. Gold-labeled amyloid and fibrillar A β structures can be observed in the higher magnification electron micrographs (right panels). The amyloid load similarly increased with age in both genotypes, but highly ordered, condensed amyloids were present in *AD;lgf1r^{+/-}* cortices (arrows) but not in the cortices of their *AD* counterparts. White scale bars represent 1 μ m, black bars 200 nm.

(B) Unbiased automated image processing indicates that median intensities of regions of interest (ROIs) around the gold particles labeling A β plaques of *AD;lgf1r^{+/-}* mice (black) are significantly ($p < 0.04$) higher than the plaque intensities of age-matched *AD* animals (red), confirming the higher compaction state of A β plaques of *AD;lgf1r^{+/-}* (135 images [34,087 ROIs] of *AD* and 101 images [26,066 ROIs] of *AD;lgf1r^{+/-}* were collected and analyzed).

(C) Using an in vitro kinetic aggregation assay to assess fibril load, 12- to 13-month-old *AD;lgf1r^{+/-}* mouse brain homogenates (blue) accelerated Thioflavin-T (ThT) monitored in vitro kinetic aggregation significantly ($p = 0.035$) faster than homogenates of age-matched *AD* brains (brown), indicating more A β seeding competent assemblies in *AD;lgf1r^{+/-}* mouse brains. Inset: Statistical analysis of results obtained in (C). Error bars represent mean \pm SEM.

A β . Thus, we tested whether more soluble A β is present in *AD* compared to *AD;lgf1r^{+/-}* brain homogenates. We spun brain homogenates of seven *AD* and nine *AD;lgf1r^{+/-}* 12- to 13-month-

old mice to sediment highly aggregated A β (10,000 g for 10 min, 4°C) and quantified the lower molecular weight (MW) A β_{1-40} and A β_{1-42} levels in the soluble fractions using enzyme-linked

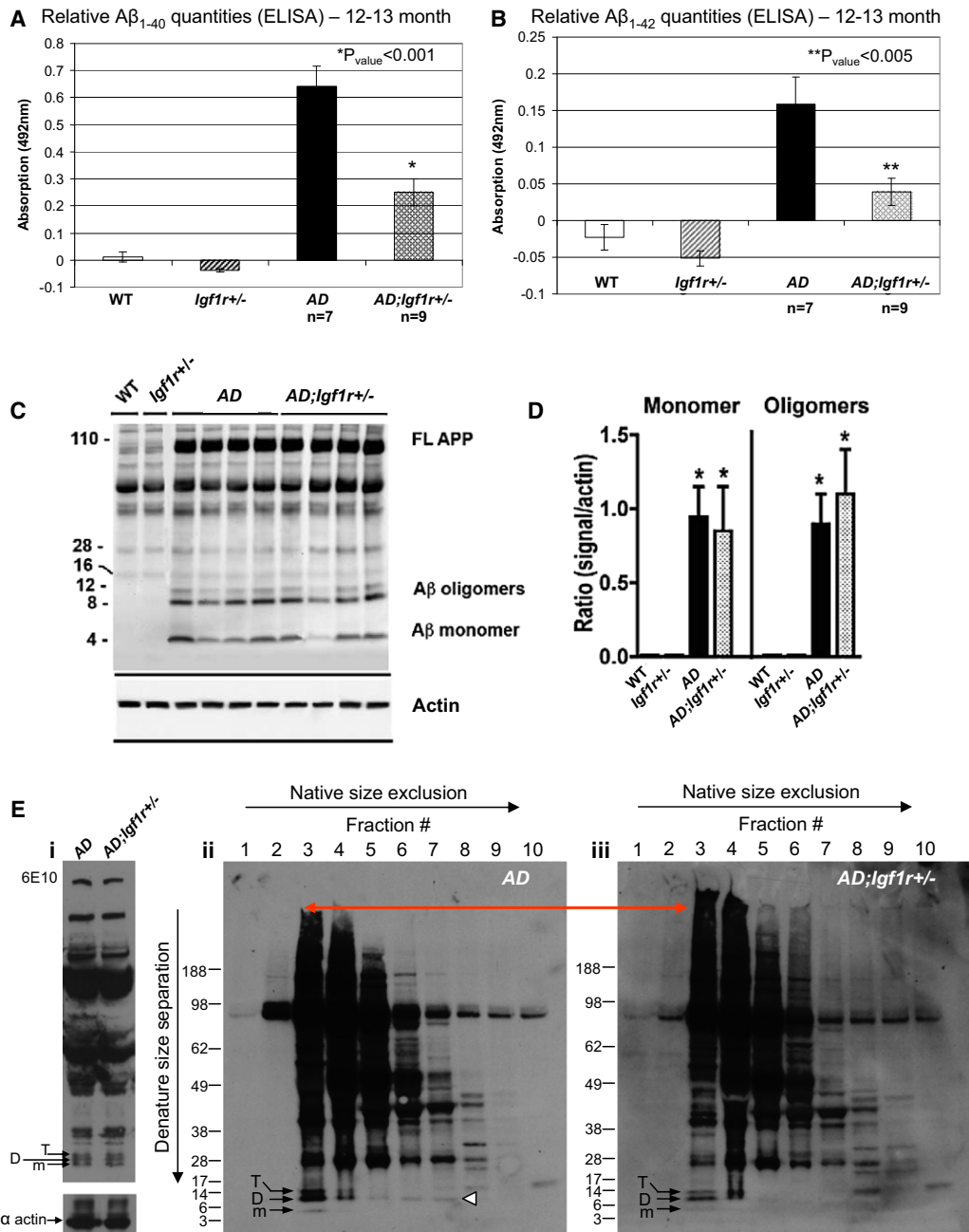


Figure 6. AD Brains Contain More Soluble A β Oligomers Than Do Brains of AD;Igf1r^{+/-} Animals

(A and B) ELISA assay detected significantly higher amounts of soluble A β_{1-40} (A) ($p < 0.001$) and A β_{1-42} (B) ($p < 0.005$) in brain homogenates of 12- to 13-month-old AD mice compared with brains of age-matched AD;Igf1r^{+/-} animals.

(C and D) Western blot analysis reveals no detectable difference in the amount of SDS-sensitive A β monomers and small oligomeric assemblies between AD and AD;Igf1r^{+/-} brain homogenates. Asterisk (*) indicates significant difference from WT or Igf1r^{+/-} mice.

(E) Native SEC indicated that A β dimers were mainly associated with large structures in brains of 16- to 17-month-old AD;Igf1r^{+/-} mice (panel iii) while more soluble in brains of age-matched AD animals (panel ii, arrowhead) (panels represent 6 AD and 6 AD;Igf1r^{+/-} animals that were analyzed). Loading of total samples onto the gel and subsequent WB analysis using 6E10, confirmed equal protein loading onto the column (panel i).

Error bars represent mean \pm SEM (A, B, and D).

immunosorbent (ELISA) assays. A β_{1-40} (Figure 6A) and A β_{1-42} (Figure 6B) levels were significantly ($p < 0.001$ and $p < 0.005$, respectively) lower in the soluble brain supernatant fractions of

AD;Igf1r^{+/-} mice compared to age-matched (12-13 month) AD animals. No such differences could be detected in the amounts of soluble A β_{1-40} among young mice (Figure S7A, $p = 0.126$).

Next, we tested whether SDS-soluble A β oligomeric content and total quantities were affected by reduced IGF-1 signaling. Four *AD* and 4 *AD;Igf1r^{+/-}* mouse brains of 12- to 13-month-old mice were subjected to an A β oligomer preparation protocol (Bar-On et al., 2006) followed by SDS-PAGE and western blot (WB) analysis. Surprisingly, the SDS-soluble A β oligomer content, and total quantities and amounts of APP were indistinguishable in the total brain homogenates (Figures 6C and 6D) of *AD* and of *AD;Igf1r^{+/-}* mice (no oligomers could be detected in cytosolic fractions; Figure S7B). The difference between the oligomer analysis results and the marked difference in the pool of nonaggregated A β species among *AD;Igf1r^{+/-}* and *AD* animals observed by the ELISA assays (Figures 6A and 6B) suggests that the oligomeric A β assemblies are SDS sensitive. To test this, we employed size-exclusion chromatography (SEC) to analyze the native composition of A β assemblies in the brains of *AD* and *AD;Igf1r^{+/-}* mice. Brains of *AD;Igf1r^{+/-}* and *AD* mice were homogenized and prepared as done for the ELISA assays to preserve macromolecular structural integrity. Equal amounts of cleared homogenates (Figure 6E, panel i) were loaded onto a size-exclusion column, and 20 fractions were collected, lyophilized, resuspended, and loaded onto SDS gels. A β assemblies were visualized using WB and A β antibody (6E10). Notably, higher MW assemblies were observed in the *AD;Igf1r^{+/-}* (see red reference line) reflecting that they were larger to begin with and/or that they were more SDS resistant (Figure 6E, panel iii, fraction 3) (for size exclusion standard see Figure S7, C and D). The apparent dimer band resulting from SDS mediated denaturation of much larger aggregates is not observable in the *AD;Igf1r^{+/-}* SEC fractions (Figure 6E, panel iii), but is observable in the *AD* mouse fractions, (Figure 6E, panel ii, fractions 5–7, open arrowhead). This proposes that in the *AD;Igf1r^{+/-}* brains, A β fibrils are denser, more SDS resistant and more efficiently prevent the release of potentially toxic oligomeric species. Since toxicity has been previously associated with the capacity of high-MW assemblies to fragment (Shankar et al., 2008), prior correlations between the appearance of small SDS-stabilized A β species and neurotoxicity may reflect this. The data obtained from the microscopic analyses, ELISA and in vitro assays suggest that the conversion of oligomers into denser, higher MW, more SDS-resistant aggregates is part of the process that protects against proteotoxicity in the *AD;Igf1r^{+/-}* animals.

DISCUSSION

By comparing behavioral and pathological aspects of Alzheimer's-like disease in the *AD* and *AD;Igf1r^{+/-}* mice, we found that reduced IGF-1 signaling notably protects mice from proteotoxicity associated with the expression of the AD-linked human peptide, A β . Light and electron microscopy, as well as in vitro kinetic aggregation, ELISA, and SEC assays, all indicate that reduced IGF-1 signaling induces the assembly of A β into densely packed, larger fibrillar structures late in life. The observation that the protected *AD;Igf1r^{+/-}* mice form SDS stable A β assemblies, making it more difficult to generate presumably toxic A β dimers (Shankar et al., 2008), suggests that an active mechanism converts oligomers into densely packed aggregates of lower toxicity that protect the *AD;Igf1r^{+/-}* mice from proteotoxicity. This

hypothesis is consistent with results obtained in the A β worm model, where reduced insulin/IGF signaling protected worms from A β -associated toxicity while increasing the formation of high-MW A β aggregates (Cohen et al., 2006).

How can increased A β aggregation protect against proteotoxicity? Highly aggregated A β is thought to bear lower toxicity in comparison to oligomers (Haass and Selkoe, 2007). Accordingly, enhanced fibrillization can reduce A β toxicity in an AD-murine model (Cheng et al., 2007). Furthermore, results from long-term potentiation assays show that highly aggregated A β bears lower toxicity than small oligomers (Shankar et al., 2008). Intriguingly, the release of small oligomers, most notably dimers, from large A β assemblies (fibrils) by chemical extraction increases toxicity. In support of the hypothesis that accelerated aggregation can be protective is provided by the discoveries that the cellular chaperones HSP104 (Shorter and Lindquist, 2004) and TRiC (Behrends et al., 2006), both known to disrupt toxic protein aggregates can also mediate protection by accelerating aggregation when the concentration of the aggregating protein exceeded a threshold level. These studies raise the prospect that the creation of densely packed, large A β assemblies protects *AD;Igf1r^{+/-}* mice from proteotoxicity by trapping and storing highly toxic small aggregate structures. If active aggregation protects from A β toxicity, such protective mechanism might be expected to be negatively regulated by the IGF signaling pathway. In the worm, this activity is mediated, at least in part, by the FOXO transcription factor DAF-16 (Cohen et al., 2006), which is negatively regulated by the IIS receptor DAF-2. The FOXO gene family is highly conserved in mammals, is expressed in neurons, and is required for neuronal survival under stress (Lehtinen et al., 2006), suggesting that FOXO transcription factors are also mediators of the reduced IGF signaling protective effect in mammals.

It is likely that reduced IGF signaling ameliorates A β proteotoxicity by mechanisms in addition to A β dense fibril formation. The observation that *Igf1r^{+/-}* mice exhibit increased resistance to oxidative stress (Holzenberger et al., 2003) raises the possibility that reduced IGF-1 signaling enhances the neuronal counter proteotoxic capabilities by enhancing the levels of enzymes that protect against oxidative stress proposed to be involved in AD-associated brain damage (Fukui et al., 2007). This is supported by the observation that the production of reactive oxygen species is reduced in brains of *Igf1r^{+/-}* mice compared with their WT counterparts following MPTP treatment known to induce a Parkinson's disease-like phenotype (Nadjar et al., 2008). Moreover, overexpression of mitochondrial-targeted catalase promotes longevity of mice (Schriner et al., 2005). An alternative model suggests that increased neuronal resilience associated with reduced IGF signaling is promoted by enhanced DNA repair capabilities. It is reasonable to speculate that the histone deacetylase SIRT1, an aging regulator (Ghosh, 2008) that plays roles in the maintenance of genomic stability (Oberdoerffer et al., 2008) and regulates HSF1 (Westerheide et al., 2009), may also be a mediator of the reduced IGF signaling protective effect in the *AD;Igf1r^{+/-}* mice. The complexity and variety of effects mediated by FOXO (Partridge and Bruning, 2008) propose that reduced IGF signaling orchestrates an array of counter proteotoxic activities including A β hyperaggregation,

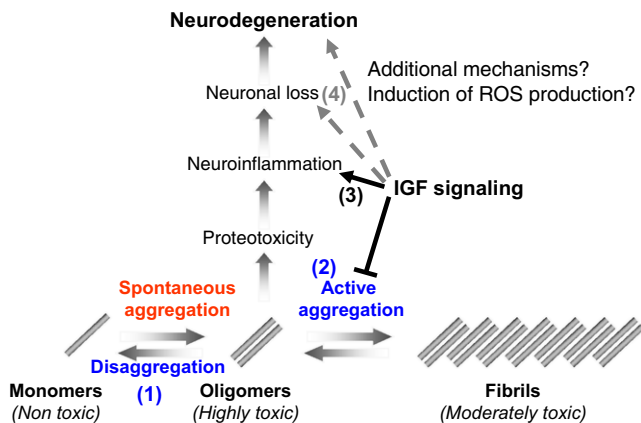


Figure 7. IGF-1 Signaling Can Play Several Roles in Mitigating the Toxicity of A β

The digestion of APP creates A β monomers that spontaneously aggregate to form toxic oligomers *in vivo*. At least two biological mechanisms can detoxify A β oligomers: (1) conversion of toxic oligomers into monomers (disaggregation), and (2) conversion of toxic oligomers into less toxic, larger structures (active aggregation). Within scenario 1, IGF-1 signaling normally functions to reduce protein disaggregases. Therefore, reduction of IGF-1 signaling would result in less oligomers and more monomeric forms of A β due to the activation of protein disaggregases. Our results are inconsistent with this scenario because we find less oligomers, but equal amounts of monomeric A β . Alternatively, in scenario 2, IGF-1 signaling could normally function to reduce protective protein aggregates that convert toxic species into larger, less toxic forms. Thus, reduced IGF-1 signaling elevates aggregase activity that in turn reduces the load of toxic oligomers and increases the compaction of less toxic fibrils. In support of scenario 2, we observed less soluble oligomers and highly compact amyloid plaques in *AD;Igf1^{+/-}* animals. Alternatively, (3) IGF-1 signaling could promote proteotoxicity and neuroinflammation in response to toxic A β assemblies. Our results are also consistent with this proposed mechanism as we observed much less neuroinflammation in the brains of protected *AD;Igf1^{+/-}* animals. Yet this lower inflammation rate could be directly related to the reduction of A β oligomers in these animals by increased aggregates. In scenario 4, reduction of toxic secondary factors, such as reactive oxygen species (ROS), might synergize with the production of toxic A β assemblies to promote neuronal loss. Consistent with this mechanism, *Igf1^{+/-}* mice are much more resistant to oxidative damage than wild-type mice. Taken together, IGF-1 signaling could impinge at multiple steps on the path to neuronal loss and neurodegeneration in response to A β production and none of the interventions are mutually exclusive. Our data are most consistent with a model in which reduced IGF-1 signaling reduces the load of toxic A β structures, presumably dimers, which results in higher compaction of plaques, reduced neuroinflammation, and reduced neuronal loss.

counter oxidation activities, and presumably other yet to be defined mechanisms (Figure 7). Further research is required to elucidate whether mammalian FOXO family members play roles in the protective mechanism toward AD.

The A β hyperaggregation observed in protected *AD;Igf1^{+/-}* mouse brains suggested that A β plaques would be visible in the cortex of these animals at younger ages compared to their unprotected AD counterparts, however, this was not evident in our analysis. This is likely due to other mechanisms of protein homeostasis being effective early in life, such as the disaggregase and degradation activity regulated by HSF-1, as observed in the worm (Cohen et al., 2006). In this view, the protective disaggregation/degradation and hyperaggregation mecha-

nisms may be temporally distinct. Active hyperaggregation may only be invoked once the primary disaggregation machinery can no longer effectively clear toxic A β species as a consequence of aging or an extrinsic stress. It will be interesting to evaluate whether one or more of the four HSF genes in the mouse are involved in protecting the brain from A β toxicity throughout life, and whether FOXO activity becomes prominent later in life.

There is an apparent contradiction between the data presented herein and earlier reports that IGF infusion protects rats (Carro et al., 2002) and mice (Carro et al., 2006) from A β proteotoxicity and that IGF-1R blockade induced neurological disease in rats (Carro et al., 2006). The presence of feedback-signaling events that respond to the sudden increase in IGF concentration by tuning down the responsiveness of the IGF signaling cascade over time could explain why IGF infusion is protective against AD-like pathology (Cohen and Dillin, 2008). This explanation is supported by many observations. For example, long-lived female human centenarians have high serum IGF-1 levels, but low IGF-1R activity, leading to reduced IGF signaling (Suh et al., 2008). Therefore, high IGF-1 levels do not necessarily correlate with increased downstream activity over a prolonged time. Additionally, AD patients have lower than normal serum insulin concentrations, but higher than normal CSF insulin levels (Craft et al., 1998). These studies raise the prospect that insulin and IGF signaling are regulated in a tissue-specific manner, and suggest that peripheral IGF infusion may lead to reduced IGF signaling in the brain (Cohen and Dillin, 2008).

The data presented here demonstrate that reduced IGF-1R signaling results in a profound reduction in the toxicity associated with A β expression in the brains of mice. The formation of larger and denser A β aggregates that appear to be more SDS resistant in the *AD;Igf1^{+/-}* mice suggests that this is one core protective activity regulated at least in part by IGF-1R signaling, much like the disaggregase activity reported previously (Cohen et al., 2006). The indication that reduced IIS is protective in nematodes and mammals stresses that manipulation of the highly conserved IGF signaling pathway, and its downstream components, is promising for the development of novel neurodegeneration and proteotoxicity therapies.

EXPERIMENTAL PROCEDURES

Mouse Strains and Genotyping

AD-model male mouse expressing a mutant chimeric mouse/human APP_{swE} and a mutant human presenilin 1 (Delta E9) both driven by the prion protein promoter was purchased from Jackson laboratory (strain B6C3-Tg [APP_{swE} PSEN1 dE9] 85Dbo/J, stock number 004462).

Long-Lived, Compromised IIS Mice

Males harboring only one *Igf1r* copy (S129 background [Holzenberger et al., 2003]) were obtained from Dr. Jeffery Friedman (TSRI, La Jolla, CA). Males of both strains were crossed for three generations with "wild-type" 129 females (Jackson laboratories, strain 129Xi/SvJ, stock number 000691), to set up two separate colonies. Mice of each colony were backcrossed for additional two generations. Next, *Igf1^{+/-}* males were crossed with AD females for three generations to generate the experimental mice.

DNA was purified from biopsies of mouse tails and subjected to PCR. APP_{swE} and PS1 Δ E9 were amplified as directed by the Jackson Laboratories. *Igf1r* was amplified using the following primers: forward: GTATAGTCCTA GAGGCC; reverse: GTTCTGGCAGAAAACATGG.

Western Blot Analysis

Brains were dissected, homogenized, and divided by ultracentrifugation (100,000 g, 1 hr, 4°C) into cytosolic and membrane (particulate) fractions. For WB analysis, 15 µg per lane of cytosolic and particulate fractions, assayed by the Lowry method, were loaded into 10% SDS-PAGE gels and blotted onto nitrocellulose paper. Blots were incubated O/N with antibodies against APP/Aβ (6E10), Aβ (82E1), and C terminus APP (CT-15, courtesy of Dr. Ed Koo). Next, membranes were incubated with secondary antibodies tagged with horseradish peroxidase (1:5000, Santa Cruz Biotechnology, Inc., Santa Cruz, CA), visualized by enhanced chemiluminescence and analyzed with a Versadoc XL imaging apparatus (Bio-Rad, Hercules, CA). Actin served as a loading control.

Rota Rod

Locomotion was tested using Rota Rod system (EconoMex, Columbus Instruments, Columbus, OH). Four mice were placed at a time on the rotating beam set to accelerate at 0.2 rpm/s.

Time from start until each mouse fell off was recorded. Each mouse was trained 1 day for five times prior to the experiment. Each mouse was tested five times a day, for 4 sequential days (total of 20 measurements/mouse/age). At least 12 animals (males and females) per genotype were used in each time point (Supplemental Statistical Data).

Morris Water Maze

The Morris water maze was conducted as described previously (Jensen et al., 2005). Briefly, 11- to 15-month-old mice of the four genotypes were placed one animal per cage and numbered randomly to avoid genotype identification during the experiment. A plastic tank 120 cm in diameter was filled with room temperature (RT) water (23°C), which was made opaque with white nontoxic paint. A transparent platform (8 cm × 12 cm) was located in the center of one of the four virtually divided quadrants and was submerged 0.5 cm below the water surface to be invisible. Distal cues were provided in all experiments as spatial references. Mice were let swim until platform was found or for a maximum of 60 s. Mice were allowed to rest on the platform for 15 s between trials. In all experimental settings we utilized a video tracking system (Ethovision; Noldus Information Technology, Leesburg, VA) to record and analyze the swimming path, swim velocity, time taken to reach the platform (latency), and time spent in each quadrant. The experiments were performed at the following order: cued platform (4 sequential days), hidden platform (4 sequential days), probe trial (1 day). The number of animals used was 13 (WT), 12 (*Igf1r^{+/-}*), 8 (*AD*), and 15 (*AD;Igf1r^{+/-}*).

Cued Platform

For the cued version of water maze testing, the platform was located 0.5 cm below the opaque water level but made clearly visible to the mouse by locating a 15 cm high stick carrying a dotted flag (3 cm × 4 cm) on the platform. The platform location was fixed throughout the experiment. The mice were released from four different locations around the water tank.

Hidden Platform

The platform was located at the same location used for the cued platform experiment, 0.5 cm below the opaque water level but without the dotted flag, to be invisible. The mice were released from four different locations around the tank. Time of latency, swim velocity, path length, and time spent at each quadrant were recorded.

Probe Trial

The platform was removed and the mice were allowed to swim for 40 s. The time spent in each quadrant and in the previous platform location, number of crossing the area where the platform was previously located, swim velocity, and path length were recorded.

Size-Exclusion Chromatography

A Superdex 75 10/300 GL column (Cat # 17-5174-01 GE Healthcare, Uppsala Sweden) attached to an AKTA FPLC system was used to separate Aβ oligomers from mouse brains. Column was calibrated using low MW calibration kit (GE Healthcare cat # 28-4038-41). Then 250 µl 10% (w/v) mouse brain

homogenate (in PBS) was injected into the column and eluted with 50 mM ammonium acetate (pH 8.5) at flow rate of 0.5 ml/min. Twenty 1 ml fractions were collected, lyophilized, resuspended in 120 µl PBS and 40 µl LDS sample buffer, boiled for 10 min, and separated on 4%–12% Bis-Tris gels as described above.

Morphological and Postembedding Immunoelectron Microscopy

WT, *Igf1r^{+/-}*, *AD*, and *AD;Igf1r^{+/-}* mice were sacrificed at the indicated ages. A piece of cortex from each mouse brain was fixed for 24 hr in cold 2% paraformaldehyde and 0.25% glutaraldehyde in PBS followed by washing in PBS and postfixed in 1% osmium tetroxide in PBS. The samples were washed in PBS and dehydrated in graded ethanol solutions followed by propylene oxide and embedded in Epon/Araldite mixture (Cat # 13940, Electron Microscopy Sciences, Hatfield, PA). The polymerized resin was sectioned (70 nm) using a diamond knife (Diatome, Hatfield, PA) and mounted on uncoated 400 mesh nickel grids (Cat# G400-Ni, Electron Microscopy Sciences) for immunolabeling. Antigen retrieval was performed using sodium m-periodate-saturated aqueous solution for 10 min followed by TBS (50 mmol/l Tris-HCl, 150 mmol/l NaCl [pH 7.4]) wash. Sections were background blocked in 3% bovine serum albumin (BSA) in TBS for 30 min followed by an overnight incubation in primary Aβ₁₋₄₂ affinity purified polyclonal rabbit antibody, which recognizes the C terminus of the peptide (Cat # AB5078P Chemicon-Millipore, Temecula, CA) 1:50 in 1% BSA in TBS at RT. Sections were washed 3 times in TBS and blocked in 3% BSA in TBS for 30 min followed by 2 hr incubation in protein A conjugated to 10nm gold particles (Cat # EM PAG10 BB International, Cardiff, UK) diluted 1:100 in 1% BSA in TBS at RT, rinsed three times in TBS, three times in H₂O, and air dried. Higher contrast was achieved with 2% uranyl acetate in 50% ethanol for 10 min and in Reynold's lead citrate solution (120 mmol/l sodium citrate, 25 mmol/l lead citrate [pH 12]) for 1.5 min. The specimens were studied in a Jeol 100CX electron microscope (Jeol, Akishima, Tokyo, Japan) at 100 kV. Electron micrographs were taken with a Mega View III CCD camera (Soft Imaging System GmbH, Muenster, Germany) and Analysis Pro v 3.2 digital micrograph software (Soft Imaging System GmbH). For detailed description and software for EM particle analysis, please see Supplemental Data and <http://sites.dillinlab.googlepages.com>.

In Vitro Kinetic Aβ Aggregation Assay

Aβ₁₋₄₀ peptide (10 µM in phosphate buffer: 300 mM NaCl, 50 mM Na-phosphate [pH 7.4]) was labeled with ThT (20 µM). Mouse brain homogenate was sonicated for 40 min (FS60, Fisher Scientific, Pittsburg, PA), treated with proteinase K (2h, 0.2 µg/ml), and supplemented with complete EDTA-free protease inhibitor cocktail (cat#1836170 Roche, Basel Switzerland). Three aliquots (100 µl each, total protein concentration of 10 µg/ml) were transferred into a 96-well microplate (Costar black, clear bottom) for each reaction. The plate was loaded into a Gemini SpectraMax EM fluorescence plate reader (Molecular Devices, Sunnyvale, CA), incubated at 37°C, and fluorescence (excitation at 440 nm, emission at 485 nm) was measured from the bottom at 10 min intervals, with 5 s of shaking before each reading. Half-maximal fluorescence time points (*t*₅₀) were defined as the time point at which ThT fluorescence reached the middle between pre- and postaggregation baselines. Fluorescence traces and *t*₅₀ values represent averages of at least three independent experiments.

SUPPLEMENTAL DATA

Supplemental Data include Supplemental Experimental Procedures and seven figures and can be found with this article online at [http://www.cell.com/supplemental/S0092-8674\(09\)01426-3](http://www.cell.com/supplemental/S0092-8674(09)01426-3).

ACKNOWLEDGMENTS

We thank Dr. Hyun-Eui Kim for expert assistance with size-exclusion chromatography and Dr. Gustavo Dziewczapolski for assistance with behavioral assay. We thank the McKnight Foundation (A.D.) and NIA P01 AG031097 (A.D., J.W.K., E.M.) for funding. E.C. and A.D. designed and initiated this study. E.C. crossed the mouse strains and performed the behavioral assays,

quantitative PCR, ELISA, size exclusion, and WB experiments. T.B.C. performed IHC assays. Immunoelectron microscopy was carried out by J.F.P. D.D. executed in vitro kinetic aggregation assays. P.B. performed image processing of the EM data. A.A. assisted with IHC. G.E. assisted with mice genotyping and behavioral assays. H.M.P. assisted with WB. M.H. provided *Igf1r*^{+/-} mice and expertise pertinent to *Igf1r*. E.C., A.D., J.W.K., and E.M. wrote the manuscript. A.D. and J.W.K. are founders of Proteostasis Therapeutics Inc. and disclose no conflict of interest in this study.

Received: June 6, 2009

Revised: September 11, 2009

Accepted: October 29, 2009

Published: December 10, 2009

REFERENCES

- Amaducci, L., and Tesco, G. (1994). Aging as a major risk for degenerative diseases of the central nervous system. *Curr. Opin. Neurol.* 7, 283–286.
- Bar-On, P., Rockenstein, E., Adame, A., Ho, G., Hashimoto, M., and Masliah, E. (2006). Effects of the cholesterol-lowering compound methyl-beta-cyclodextrin in models of alpha-synucleinopathy. *J. Neurochem.* 98, 1032–1045.
- Behrends, C., Langer, C.A., Boteva, R., Bottcher, U.M., Stemp, M.J., Schaffar, G., Rao, B.V., Giese, A., Kretzschmar, H., Siegers, K., et al. (2006). Chaperonin TRiC promotes the assembly of polyQ expansion proteins into nontoxic oligomers. *Mol. Cell* 23, 887–897.
- Blanchard, J., Martel, G., Guillou, J.L., Nogues, X., and Micheau, J. (2008). Impairment of spatial memory consolidation in APP(751SL) mice results in cue-guided response. *Neurobiol. Aging* 29, 1011–1021.
- Blüher, M., Kahn, B.B., and Kahn, C.R. (2003). Extended longevity in mice lacking the insulin receptor in adipose tissue. *Science* 299, 572–574.
- Carro, E., Trejo, J.L., Gomez-Isla, T., LeRoith, D., and Torres-Aleman, I. (2002). Serum insulin-like growth factor I regulates brain amyloid-beta levels. *Nat. Med.* 8, 1390–1397.
- Carro, E., Trejo, J.L., Spuch, C., Bohl, D., Heard, J.M., and Torres-Aleman, I. (2006). Blockade of the insulin-like growth factor I receptor in the choroid plexus originates Alzheimer's-like neuropathology in rodents: new cues into the human disease? *Neurobiol. Aging* 27, 1618–1631.
- Cheng, I.H., Scearce-Levie, K., Legleiter, J., Palop, J.J., Gerstein, H., Bien-Ly, N., Puolivali, J., Lesne, S., Ashe, K.H., Muchowski, P.J., et al. (2007). Accelerating amyloid-beta fibrillization reduces oligomer levels and functional deficits in Alzheimer disease mouse models. *J. Biol. Chem.* 282, 23818–23828.
- Cohen, E., Bieschke, J., Perciavalle, R.M., Kelly, J.W., and Dillin, A. (2006). Opposing activities protect against age-onset proteotoxicity. *Science* 313, 1604–1610.
- Cohen, E., and Dillin, A. (2008). The insulin paradox: aging, proteotoxicity and neurodegeneration. *Nat. Rev. Neurosci.* 9, 759–767.
- Craft, S., Peskind, E., Schwartz, M.W., Schellenberg, G.D., Raskind, M., and Porte, D., Jr. (1998). Cerebrospinal fluid and plasma insulin levels in Alzheimer's disease: relationship to severity of dementia and apolipoprotein E genotype. *Neurology* 50, 164–168.
- Farzan, M., Schnitzler, C.E., Vasilieva, N., Leung, D., and Choe, H. (2000). BACE2, a beta-secretase homolog, cleaves at the beta site and within the amyloid-beta region of the amyloid-beta precursor protein. *Proc. Natl. Acad. Sci. USA* 97, 9712–9717.
- Flachsbar, F., Caliebe, A., Kleindorp, R., Blanche, H., von Eller-Eberstein, H., Nikolaus, S., Schreiber, S., and Nebel, A. (2009). Association of FOXO3A variation with human longevity confirmed in German centenarians. *Proc. Natl. Acad. Sci. USA* 106, 2700–2705.
- Fukui, H., Diaz, F., Garcia, S., and Moraes, C.T. (2007). Cytochrome c oxidase deficiency in neurons decreases both oxidative stress and amyloid formation in a mouse model of Alzheimer's disease. *Proc. Natl. Acad. Sci. USA* 104, 14163–14168.
- Ghosh, H.S. (2008). The anti-aging, metabolism potential of SIRT1. *Curr. Opin. Investig. Drugs* 9, 1095–1102.
- Glenner, G.G., and Wong, C.W. (1984). Alzheimer's disease: initial report of the purification and characterization of a novel cerebrovascular amyloid protein. *Biochem. Biophys. Res. Commun.* 120, 885–890.
- Haass, C., and Selkoe, D.J. (2007). Soluble protein oligomers in neurodegeneration: lessons from the Alzheimer's amyloid beta-peptide. *Nat. Rev.* 8, 101–112.
- Hamos, J.E., DeGennaro, L.J., and Drachman, D.A. (1989). Synaptic loss in Alzheimer's disease and other dementias. *Neurology* 39, 355–361.
- Holzenberger, M., Dupont, J., Ducos, B., Leneuve, P., Geloën, A., Even, P.C., Cervera, P., and Le Bouc, Y. (2003). IGF-1 receptor regulates lifespan and resistance to oxidative stress in mice. *Nature* 421, 182–187.
- Jankowsky, J.L., Fadale, D.J., Anderson, J., Xu, G.M., Gonzales, V., Jenkins, N.A., Copeland, N.G., Lee, M.K., Younkin, L.H., Wagner, S.L., et al. (2004). Mutant presenilins specifically elevate the levels of the 42 residue beta-amyloid peptide in vivo: evidence for augmentation of a 42-specific gamma secretase. *Hum. Mol. Genet.* 13, 159–170.
- Jankowsky, J.L., Slunt, H.H., Ratovitski, T., Jenkins, N.A., Copeland, N.G., and Borchelt, D.R. (2001). Co-expression of multiple transgenes in mouse CNS: a comparison of strategies. *Biomol. Eng.* 17, 157–165.
- Jensen, M.T., Mottin, M.D., Cracchiolo, J.R., Leighty, R.E., and Arendash, G.W. (2005). Lifelong immunization with human beta-amyloid (1-42) protects Alzheimer's transgenic mice against cognitive impairment throughout aging. *Neuroscience* 130, 667–684.
- Kenyon, C., Chang, J., Gensch, E., Rudner, A., and Tabtiang, R. (1993). A *C. elegans* mutant that lives twice as long as wild type. *Nature* 366, 461–464.
- Kimura, K.D., Tissenbaum, H.A., Liu, Y., and Ruvkun, G. (1997). *daf-2*, an insulin receptor-like gene that regulates longevity and diapause in *Caenorhabditis elegans*. *Science* 277, 942–946.
- King, D.L., and Arendash, G.W. (2002). Behavioral characterization of the Tg2576 transgenic model of Alzheimer's disease through 19 months. *Physiol. Behav.* 75, 627–642.
- Lehtinen, M.K., Yuan, Z., Boag, P.R., Yang, Y., Villen, J., Becker, E.B., DiBacco, S., de la Iglesia, N., Gygi, S., Blackwell, T.K., et al. (2006). A conserved MST-FOXO signaling pathway mediates oxidative-stress responses and extends life span. *Cell* 125, 987–1001.
- Lesne, S., Koh, M.T., Kotilinek, L., Kaye, R., Glabe, C.G., Yang, A., Gallagher, M., and Ashe, K.H. (2006). A specific amyloid-beta protein assembly in the brain impairs memory. *Nature* 440, 352–357.
- Link, C.D. (1995). Expression of human beta-amyloid peptide in transgenic *Caenorhabditis elegans*. *Proc. Natl. Acad. Sci. USA* 92, 9368–9372.
- Mancardi, G.L., Liwnicz, B.H., and Mandybur, T.I. (1983). Fibrous astrocytes in Alzheimer's disease and senile dementia of Alzheimer's type. *Acta Neuropathol.* 61, 76–80.
- Masliah, E., and Rockenstein, E. (2000). Genetically altered transgenic models of Alzheimer's disease. *J. Neural Transm. Suppl.* 59, 175–183.
- Morley, J.F., Brignull, H.R., Weyers, J.J., and Morimoto, R.I. (2002). The threshold for polyglutamine-expansion protein aggregation and cellular toxicity is dynamic and influenced by aging in *Caenorhabditis elegans*. *Proc. Natl. Acad. Sci. USA* 99, 10417–10422.
- Nadjar, A., Berton, O., Guo, S., Leneuve, P., Dovero, S., Diguët, E., Tison, F., Zhao, B., Holzenberger, M., and Bezard, E. (2008). IGF-1 signaling reduces neuro-inflammatory response and sensitivity of neurons to MPTP. *Neurobiol. Aging* 30, 2021–2130.
- Oberdoerffer, P., Michan, S., McVay, M., Mostoslavsky, R., Vann, J., Park, S.K., Hartlerode, A., Stegmüller, J., Hafner, A., Loerch, P., et al. (2008). SIRT1 redistribution on chromatin promotes genomic stability but alters gene expression during aging. *Cell* 135, 907–918.
- Partridge, L., and Bruning, J.C. (2008). Forkhead transcription factors and aging. *Oncogene* 27, 2351–2363.
- Reiserer, R.S., Harrison, F.E., Syverud, D.C., and McDonald, M.P. (2007). Impaired spatial learning in the APP^{Swe} + PSEN1^{DeltaE9} bigenic mouse model of Alzheimer's disease. *Genes Brain Behav.* 6, 54–65.

- Scheff, S.W., DeKosky, S.T., and Price, D.A. (1990). Quantitative assessment of cortical synaptic density in Alzheimer's disease. *Neurobiol. Aging* 11, 29–37.
- Schriner, S.E., Linford, N.J., Martin, G.M., Treuting, P., Ogburn, C.E., Emond, M., Coskun, P.E., Ladiges, W., Wolf, N., Van Remmen, H., et al. (2005). Extension of murine life span by overexpression of catalase targeted to mitochondria. *Science* 308, 1909–1911.
- Selkoe, D.J. (2004). Alzheimer disease: mechanistic understanding predicts novel therapies. *Ann. Intern. Med.* 140, 627–638.
- Shankar, G.M., Li, S., Mehta, T.H., Garcia-Munoz, A., Shepardson, N.E., Smith, I., Brett, F.M., Farrell, M.A., Rowan, M.J., Lemere, C.A., et al. (2008). Amyloid-beta protein dimers isolated directly from Alzheimer's brains impair synaptic plasticity and memory. *Nat. Med.* 14, 837–842.
- Shorter, J., and Lindquist, S. (2004). Hsp104 catalyzes formation and elimination of self-replicating Sup35 prion conformers. *Science* 304, 1793–1797.
- Suh, Y., Atzmon, G., Cho, M.O., Hwang, D., Liu, B., Leahy, D.J., Barzilai, N., and Cohen, P. (2008). Functionally significant insulin-like growth factor I receptor mutations in centenarians. *Proc. Natl. Acad. Sci. USA* 105, 3438–3442.
- Tatar, M., Kopelman, A., Epstein, D., Tu, M.P., Yin, C.M., and Garofalo, R.S. (2001). A mutant *Drosophila* insulin receptor homolog that extends life-span and impairs neuroendocrine function. *Science* 292, 107–110.
- Westerheide, S.D., Ankar, J., Stevens, S.M., Jr., Sistonen, L., and Morimoto, R.I. (2009). Stress-inducible regulation of heat shock factor 1 by the deacetylase SIRT1. *Science* 323, 1063–1066.
- Westerman, M.A., Cooper-Blacketer, D., Mariash, A., Kotilinek, L., Kawarabayashi, T., Younkin, L.H., Carlson, G.A., Younkin, S.G., and Ashe, K.H. (2002). The relationship between Abeta and memory in the Tg2576 mouse model of Alzheimer's disease. *J. Neurosci.* 22, 1858–1867.
- Willcox, B.J., Donlon, T.A., He, Q., Chen, R., Grove, J.S., Yano, K., Masaki, K.H., Willcox, D.C., Rodriguez, B., and Curb, J.D. (2008). FOXO3A genotype is strongly associated with human longevity. *Proc. Natl. Acad. Sci. USA* 105, 13987–13992.
- Wirhiths, O., Breyhan, H., Marcello, A., Cotel, M.C., Bruck, W., and Bayer, T.A. (2008). Inflammatory changes are tightly associated with neurodegeneration in the brain and spinal cord of the APP/PS1KI mouse model of Alzheimer's disease. *Neurobiol. Aging*, in press. Published online July 26, 2008. 10.1016/j.neurobiolaging.2008.06.011.
- Wolfe, M.S., Xia, W., Ostaszewski, B.L., Diehl, T.S., Kimberly, W.T., and Selkoe, D.J. (1999). Two transmembrane aspartates in presenilin-1 required for presenilin endoproteolysis and gamma-secretase activity. *Nature* 398, 513–517.